



Regulatory Control of Microglial Phagocytosis by Estradiol and Prostaglandin E₂ in the Developing Rat Cerebellum

Miguel Perez-Pouchoulen¹ · Stacey J. Yu¹ · Clinton R. Roby¹ · Nicole Bonsavage¹ · Margaret M. McCarthy¹

Published online: 21 August 2019

© Springer Science+Business Media, LLC, part of Springer Nature 2019

Abstract

Microglia are essential to sculpting the developing brain, and they achieve this in part through the process of phagocytosis which is regulated by microenvironmental signals associated with cell death and synaptic connectivity. In the rat cerebellum, microglial phagocytosis reaches its highest activity during the third postnatal week of development but the factors regulating this activity are unknown. A signaling pathway, involving prostaglandin E₂ (PGE₂) stimulation of the estrogen synthetic enzyme aromatase, peaks during the 2nd postnatal week and is a critical regulator of Purkinje cell maturation. We explored the relationship between the PGE₂-estradiol pathway and microglia in the maturing cerebellum. Toward that end, we treated developing rat pups with pharmacological inhibitors of estradiol and PGE₂ synthesis and then stained microglia with the universal marker Iba1 and quantified microglia engaged in phagocytosis as well as phagocytic cups in the vermis and cerebellar hemispheres. Inhibition of aromatase reduced the number of phagocytic cups in the vermis, but not in the cerebellar hemisphere at postnatal day 17. Similar results were found after treatment with nimesulide and indomethacin, inhibitors of the PGE₂-producing enzymes cyclooxygenase 1 and 2. In contrast, treatment with estradiol or PGE₂ had little effect on microglial phagocytosis in the developing cerebellum. Thus, endogenous estrogens and prostaglandins upregulate the phagocytic activity of microglia during a select window of postnatal cerebellar development, but exogenous treatment with these same signaling molecules does not further increase the already high levels of phagocytosis. This may be due to an upper threshold or evidence of resistance to exogenous perturbation.

Keywords Estrogen · Prostaglandins · Cerebellar cortex · Phagocytic cups · Phagocytic markers

Introduction

Microglia, the resident macrophages of the central nervous system (CNS), are essential participants in the development of the brain and its neuronal circuits. During development, microglia both remove and promote the formation of dendritic spines, synapses, and live and dead cells to establish connections between neurons [1–8]. One mechanism by which microglia efficiently mediate these diverse effects is phagocytosis, a process in which cell particles or entire cell nuclei are engulfed and ingested [9]. Microglia can be classified based on morphology to give insight into activation state [10–12]. Microglia with an amoeboid-like shape are considered the

most activated as they produce higher levels of inflammatory mediators. As microglia become less activated, they become increasingly ramified. Both ramified and non-ramified microglia are capable of phagocytosis [2, 5, 13–16]. Local environmental signals, associated with chemotaxis, cell death, injury, inflammation, as well as synaptic connectivity, can all regulate microglial phagocytosis [1, 2, 4, 17, 18]. Moreover, the phagocytic profile of microglia varies according to developmental stage, brain region, and sex [5, 16, 19]. In this regard, microglial phagocytosis has been mainly studied under infectious or injury conditions. However, how developmental signals such as hormonal milieu impact microglial phagocytosis in the healthy CNS is poorly understood.

The signaling molecules estradiol and prostaglandin E₂ (PGE₂) regulate each other's synthesis in a region dependent manner and play crucial role during brain development [20, 21]. In the preoptic area, estradiol promotes PGE₂ production [22] while in the cerebellum, the opposite is true, PGE₂ promotes estradiol synthesis [20]. Both signaling molecules also directly regulate fundamental biological processes such as neuronal survival, neurogenesis, apoptotic cell death,

✉ Miguel Perez-Pouchoulen
mpouchoulen@som.umaryland.edu

¹ Department of Pharmacology, University of Maryland School of Medicine, 670 W. Baltimore Street, HSFIII 9-130, Baltimore, MD 21201, USA

spinogenesis, and synaptogenesis [20, 22–27]. Estradiol, the aromatized end product of testosterone, not only promotes masculinization of many neuroanatomical end points in the developing rodent brain, but also provides trophic support and neuroprotective effects that may or may not be influenced by sex [23]. Therefore, changes in estradiol or PGE₂ levels during development can lead to substantial cellular, morphological, and behavioral abnormalities later in life [22, 28–30]. Both signaling molecules interact with the immune system [31–36], and microglia are responsive to estrogens and prostaglandins [16, 37–41].

Previously, we conducted a morphological profile of microglia in the developing rat cerebellum and found that ramified microglia were highly phagocytic and that this activity peaked during the third postnatal week in the granular layer (GL), but not in the molecular layer (ML) of the cerebellar cortex [5]. These phagocytic cups, defined as that are cup-shaped invaginations of the plasma membrane located at the end of the processes [9], were associated with apoptotic cells, suggesting involvement in the removal of dead cells as part of the maturation of the cerebellar circuit. Previous work from our lab indicated the developing cerebellum is sensitive to the actions of estrogens and prostaglandins [20, 28, 29], and previous work has shown mRNA expression of aromatase within Purkinje neurons in the postnatal developing cerebellum as well as the localization of ER α and ER β , both mRNA and protein, within Purkinje neurons and granule cells during dendritic growth and synapse formation [24, 42, 43]. Additionally, cyclooxygenase enzymes COX-1 and COX-2, involved in the synthesis of PGE₂, are present in the developing cerebellum [44, 45] and prostaglandin receptors (EP1–4) have been found in the developing cerebellum on Purkinje neurons and astrocytes [46, 47].

These observations led us to hypothesize that both estradiol and PGE₂ modify phagocytic activity of microglia in the developing cerebellum, a structure that undergoes major growth and synaptic remodeling after birth [48, 49]. We report here that both of these signaling molecules are endogenous regulators of microglia phagocytic activity, but we found no impact of treatment with exogenous estradiol or PGE₂.

Materials and Methods

Animals

Timed pregnant Sprague–Dawley rats, either purchased from Charles River or raised in our breeding colony, delivered naturally under standard laboratory conditions. The day of birth was designated postnatal day 0 (PN0), as determined by the presence of pups in the nest. All animals were housed in polycarbonate cages (20 × 40 × 20 cm) with corn cob bedding under 12:12 h reverse light/dark cycle, with ad libitum water and

food. The Institutional Animal Care and Use Committee of the University of Maryland, Baltimore approved all animal procedures. In all experiments, pups were obtained from 3 to 4 different litters and included equal number of males and females.

Cerebellum Collection and Iba1 Immunohistochemistry

Animals were deeply anesthetized with Fatal Plus (Vortech Pharmaceuticals) and transcardially perfused with 0.9% saline solution followed by 4% paraformaldehyde. The whole cerebellum was removed and post-fixed overnight in 4% paraformaldehyde, and cryoprotected with 30% sucrose until saturated, then sectioned sagittally on a cryostat (thickness = 45 μ m) and separated into vermis, left and right cerebellar hemispheres (LH and RH, respectively). Free-floating cerebellar sections were co-incubated with a polyclonal antibody against Iba1 (1:10000, Wako Chemicals) to visualize microglial cells [5]. Sections were mounted on silane-coated slides, cleared with ascending alcohol, defatted with xylene, and coverslipped with DPX mounting medium.

Morphological Identification of Phagocytic Microglia in the Cerebellar Cortex

Microglia can be classified based on their morphology which varies from an amorphous amoeboid shape to highly ramified. This shift loosely correlates with a functional state ranging from activated to surveying [5]. Here, our focus is on phagocytic microglia which we subdivided into those that are large with thick processes, have an amorphous cell body, at least two thick ramified processes, and exhibit at least one phagocytic cup versus phagocytic microglia with thin processes having a round and small cell body with at least four thin ramified processes and exhibiting at least one phagocytic cup. Phagocytic cups appear as cup-shaped invaginations of the plasma membrane, and only cups located at the tip of microglial processes with a round morphology were counted. Our goal was to discern if there was a regional difference or treatment effect on phagocytic microglia that were more activated (thick processes) versus that are primarily surveying (thin processes). Phagocytic microglia and the number of phagocytic cups were quantified independently as some microglia exhibit more than one cup. Counts were performed in the GL and ML of the cerebellar cortex, which are both well developed at PN17. Microglia in the cerebellar white matter were excluded.

Stereological Counts

We used StereoInvestigator 10 (Microbrightfield) interfaced with a Nikon Eclipse 80i microscope and an MBF Bioscience

01-MBF-2000R-F-CLR-12 Digital Camera (Color 12 BIT). A total of six counting regions in the vermis and four counting regions in the cerebellar hemisphere were assessed (Fig. 1). The counting regions represent the anterior, posterior, dorsal and ventral areas of each part of the cerebellum. Four cerebellar sections from the vermis and each cerebellar hemisphere were quantified per animal with a physical distance of 225 μm between them, reducing the likelihood of double counting microglia due to their small cell size. The optical fractionator probe method was used to estimate cell and phagocytic cup densities following stereological parameters previously standardized in our lab [5]. Iba1⁺ cells and phagocytic cups were counted at $\times 20$ magnification. The overall estimated volume of each counting region was used to normalize counts to obtain an estimation of the average density of objects of interest (e.g., phagocytic microglia, phagocytic cups), which was expressed as number/ μm^3 (relative density measurement). Experimenters were blinded to the experimental condition of the samples.

Experiment 1

Phagocytic Microglia Counting in the Vermis and in the Cerebellar Hemispheres

We previously found that microglia from the GL of the cerebellar cortex exhibit higher phagocytic activity than the ML at PN17 in the vermis [5]. In this experiment, we included both cerebellar hemispheres (Fig. 1), left and right, to determine whether these two regions of the

cerebellum show a similar phagocytic activity pattern as the vermis at PN17 (Fig. 2a). Phagocytic microglia with either thick or thin processes and phagocytic cups were counted in each region of interest ($n = 6$).

Experiment 2

Inhibition of Aromatase in the Developing Cerebellum

Neonatal rat pups ($n = 6$) were subcutaneously (s.c.) injected with the aromatase inhibitor formestane (Sigma, 5 $\mu\text{g}/0.05$ ml dissolved in sesame oil) or vehicle (sesame oil) for 5 consecutive days starting on PN8 (Fig. 3a). On PN17, pups were perfused and the cerebellums visualized for Iba1 immunohistochemistry. We counted phagocytic microglia and phagocytic cups in both GL and ML in the vermis and cerebellar hemisphere. Since no significant differences were found between the left and right cerebellar hemispheres in experiment 1, we quantified microglia in only the left cerebellar hemisphere.

Experiment 3

Inhibition of Cyclooxygenases 1 and 2 in the Developing Cerebellum

We investigated whether the inhibition of cyclooxygenases 1 and 2 (Cox-1 and Cox-2,

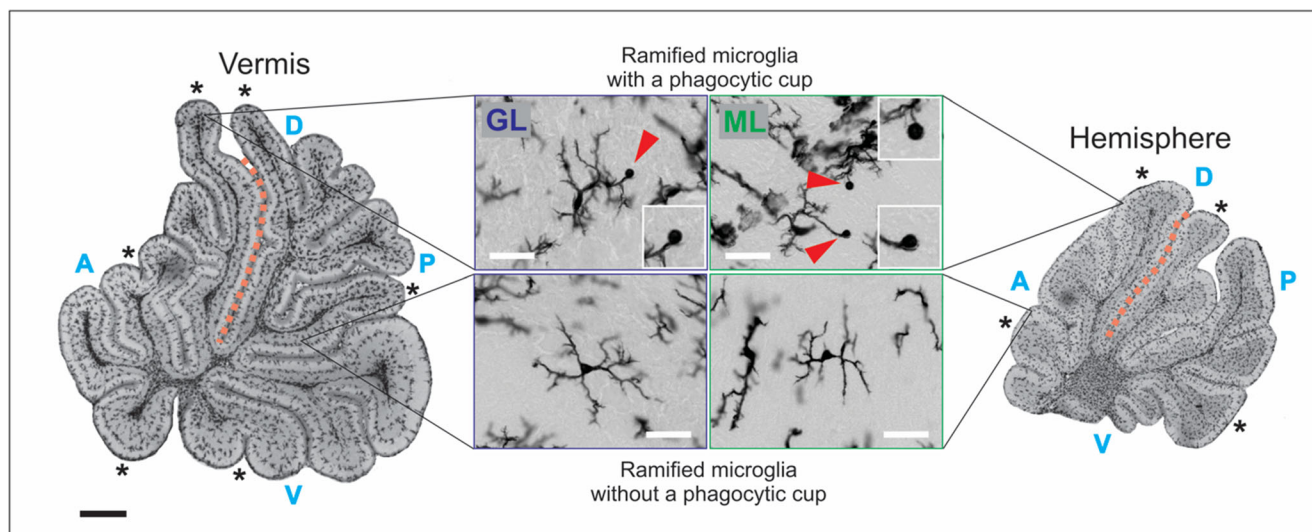


Fig. 1 Microglia staining in the developing cerebellum. Sagittal representation of the vermis (left image, scale bar = 500 μm) and the hemisphere (right image) with Iba1 staining (free floating immunohistochemistry, section thickness = 45 μm). The asterisk indicates the regions used to count microglia by stereological methods. Images in the center depict phagocytic (top image, scale bar = 25 μm) and

non-phagocytic (bottom image, scale bar = 25 μm) microglia. Phagocytic cups exhibited by microglia in the cerebellar cortex are pointed out by a red arrow head (also see insets showing a phagocytic cup with a higher magnification). GL granular layer, ML molecular layer, A anterior area, P posterior area, D dorsal area, V ventral area. Primary fissure = dotted orange line

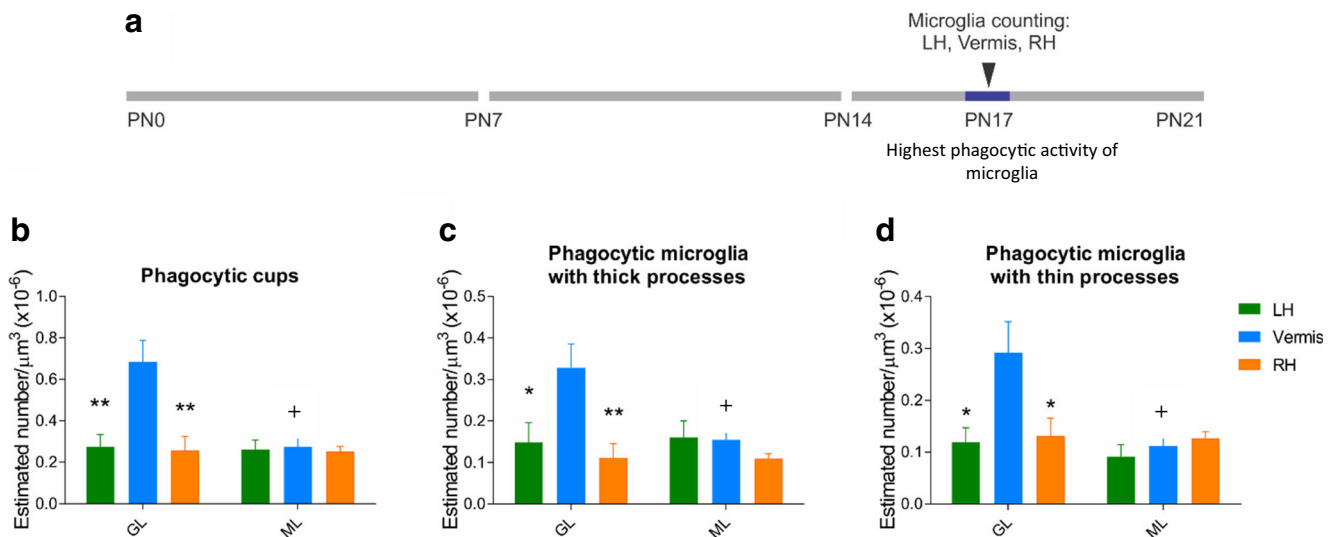


Fig. 2 Microglial phagocytosis in the vermis and hemisphere. **a** Experimental time line showing that microglia were counted on PN17 under typical developmental conditions in the three regions of the cerebellum (LH left hemisphere, RH right hemisphere). Representation of the number of phagocytic cups (**b**), phagocytic microglia with thick processes (**c**), and phagocytic microglia with thin processes (**d**) counted in

the cerebellar cortex. GL granular layer, ML molecular layer, PN postnatal day. Significant differences found in the GL are denoted by * $p < 0.05$, ** $p < 0.01$ when LH and RH are compared with the vermis. Significant differences are denoted by + $p < 0.05$ when the vermis-GL and the vermis-ML are compared

respectively), the enzymes responsible for PGE₂ synthesis, alters microglial phagocytosis on PN17 by injecting indomethacin (Cox-1 and Cox-2 inhibitor; Sigma, 25 $\mu\text{g}/0.05$ ml), nimesulide (Cox-2 inhibitor; Sigma, 50 $\mu\text{g}/0.05$ ml), or vehicle (sesame oil) into neonatal rat pups ($n = 6$) following the same experimental design described in experiment 2 (Fig. 4a). Concentrations of indomethacin and nimesulide were chosen based on previous work in our lab [29].

Experiment 4

Effect of Estradiol Treatment on the Developing Cerebellum

Pups were injected (s.c.) once a day with 17 β -estradiol-3 benzoate (Sigma, estradiol 5 $\mu\text{g}/0.05$ ml dissolved in sesame oil, $n = 6$) or vehicle (sesame oil, $n = 6$) from PN8 to PN12 (Fig. 5a) and a second cohort from PN10 to PN14 (Fig. 5e). Subsequently, on PN17, rat pups were perfused and their cerebellums visualized for Iba1 immunohistochemistry. Phagocytic microglia and phagocytic cups were counted in both GL and ML, but only in the vermis since we found significant differences for microglial phagocytosis when treated with formestane, but not the cerebellar hemisphere. Concentration of estradiol was chosen based on previous work in our lab [20].

Experiment 5

PGE₂ and Microglial Phagocytosis in the Developing Cerebellum

We explored the effect of PGE₂ by injecting 2.5 $\mu\text{g}/\mu\text{l}$ of PGE₂ directly into the cisterna magna of rat pups. These pups received a single injection of PGE₂ on PN10 and again on PN12 (3 males and 3 females for each group) (Fig. 6a), and phagocytic microglia and phagocytic cups were measured on PN17 as described above. The PGE₂ concentration was selected based on previous work in our lab showing this dose is sufficient to induce an increase in estradiol synthesis by stimulating aromatase in the cerebellum during the second postnatal week [20, 28].

Experiment 6

DHT and Microglial Phagocytosis in the Developing Cerebellum

We also investigated whether androgens affect microglial phagocytosis in the developing cerebellum by injecting dihydrotestosterone (DHT benzoate; Sigma, 5 $\mu\text{g}/0.05$ ml), an androgen that cannot be aromatized to estradiol, or vehicle (sesame oil) into neonatal rat pups (3 males and 3 females for each group) from PN10 to PN14 following the same experimental design described in experiment 4 (Fig. 5e). DHT concentration was chosen based on previous work in our lab [50].

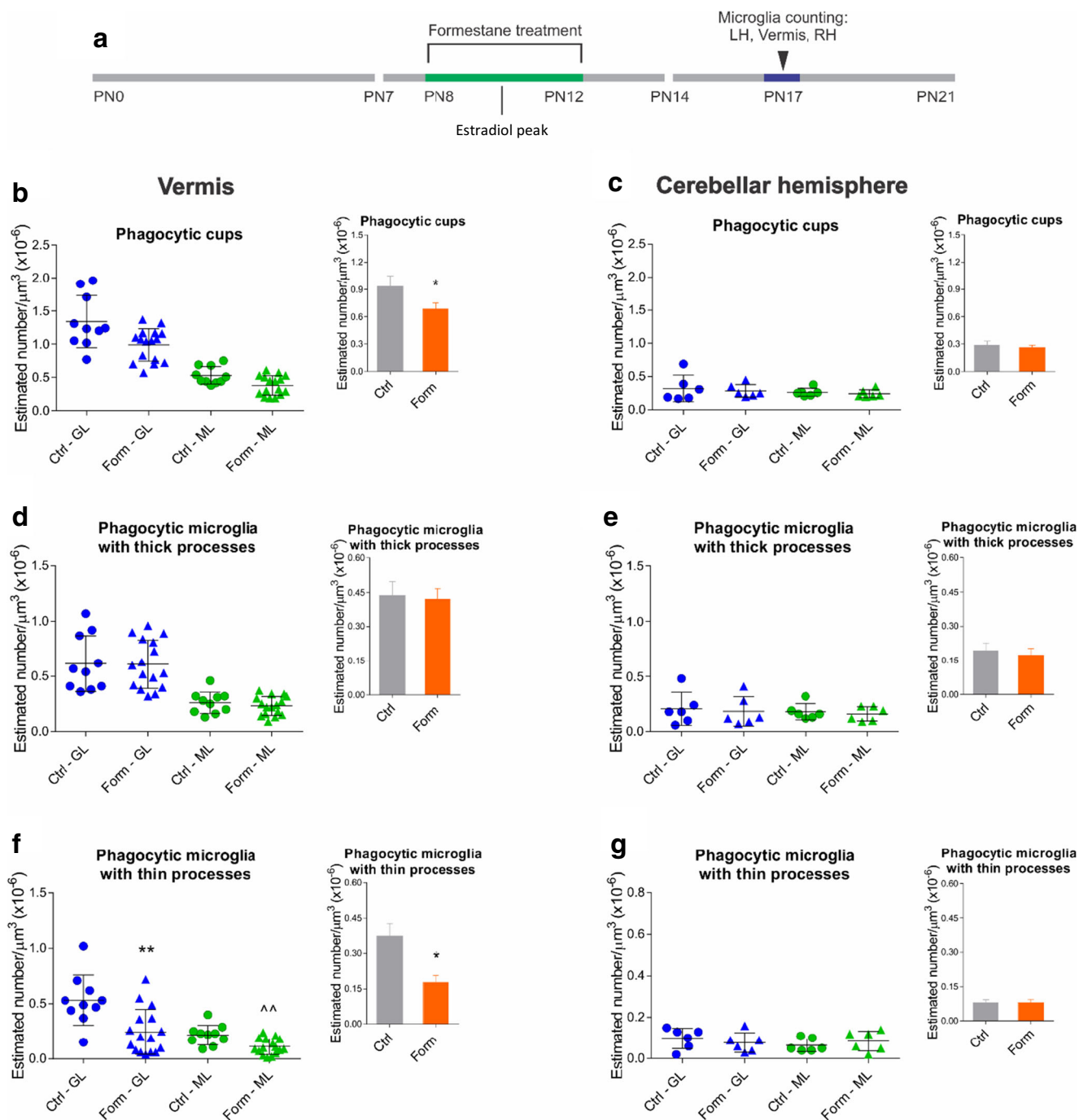


Fig. 3 Effect of formestane treatment on microglial phagocytosis in the developing cerebellum. In each panel, two graphs are presented: the individual point graph and the histogram. The latter represents the data analyzed when only treatment is considered as a main factor. **a** Experimental design showing formestane treatment interval (PN8–PN12) and microglia counting at PN17 in vermis and hemisphere. The number of phagocytic cups (**b**, $*p=0.01$), phagocytic microglia with thick processes (**d**), and phagocytic microglia with thin processes (**f**,

$*p=0.04$, $**p=0.01$ compared to Ctrl in the GL, $^{\wedge}p=0.003$ compared to Ctrl in the ML) counted in the vermis following treatment with formestane. Characterization of the number of phagocytic cups (**c**), phagocytic microglia with thick processes (**e**), and phagocytic microglia with thin processes (**g**) counted in the cerebellar hemisphere following treatment with formestane. GL granular layer, ML molecular layer, Ctrl control, Form formestane, PN postnatal day

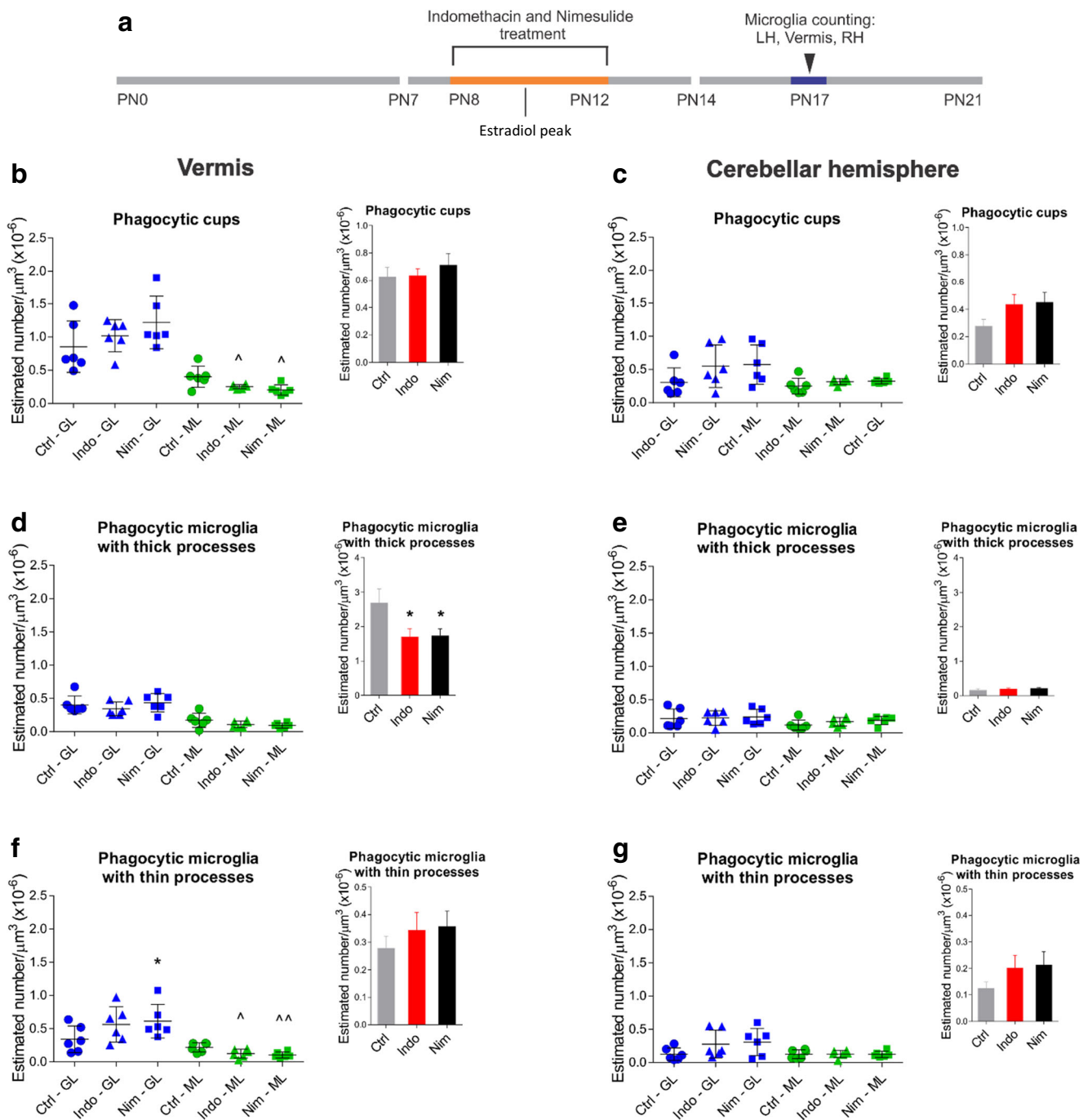


Fig. 4 Effect of indomethacin and nimesulide treatment on microglial phagocytosis in the developing cerebellum. In each panel, two graphs are presented: the individual point graph and the histogram. The latter represents the data analyzed when only treatment is considered as a main factor. **a** Experimental design illustrating indomethacin and nimesulide treatment intervals (PN8–PN12) and microglia counting at PN17 in the vermis and hemisphere. The number of phagocytic cups (**b**, $^{\wedge}p < 0.05$ compared to Ctrl in the ML), phagocytic microglia with thick processes (**d**, $*p < 0.05$, compared to Ctrl), and phagocytic microglia with thin

processes (**f**, $*p < 0.05$, compared to Ctrl in the GL, $^{\wedge}p < 0.05$, $^{\wedge\wedge}p < 0.01$ compared to Ctrl in the ML) counted in the vermis following treatment with formestane. Characterization of the number of phagocytic cups (**c**), phagocytic microglia with thick processes (**e**), and phagocytic microglia with thin processes (**g**) counted in the cerebellar hemisphere following treatment with formestane. GL granular layer, ML molecular layer, Ctrl control, Indo indomethacin, Nim nimesulide, PN postnatal day

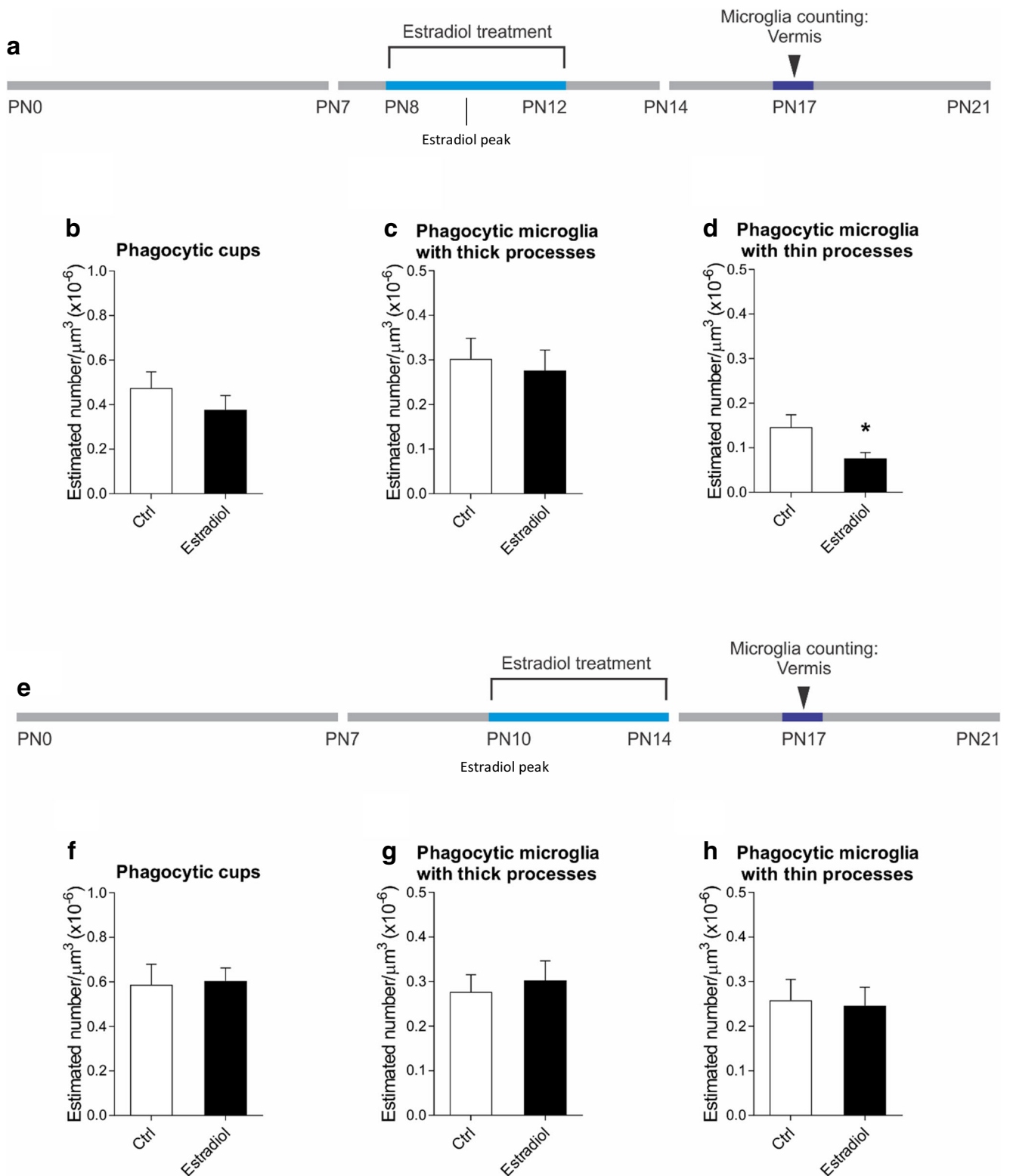


Fig. 5 Effect of estradiol treatment on microglial phagocytosis in the developing cerebellum. **a** Experimental design showing estradiol treatment interval (PN8–PN12) and microglia counting at PN17 in the vermis. The number of phagocytic cups (**b**), phagocytic microglia with thick processes (**c**), and phagocytic microglia with thin processes (**d**, $*p < 0.05$) counted in the vermis following treatment with estradiol. **e**

Experimental design showing estradiol treatment interval (PN10–PN14) and microglia counting at PN17 in the vermis. Characterization of the number of phagocytic cups (**f**), phagocytic microglia with thick processes (**g**), and phagocytic microglia with thin processes (**h**) counted in the cerebellar hemisphere following treatment with formestane. Ctrl control, EB estradiol benzoate, PN postnatal day

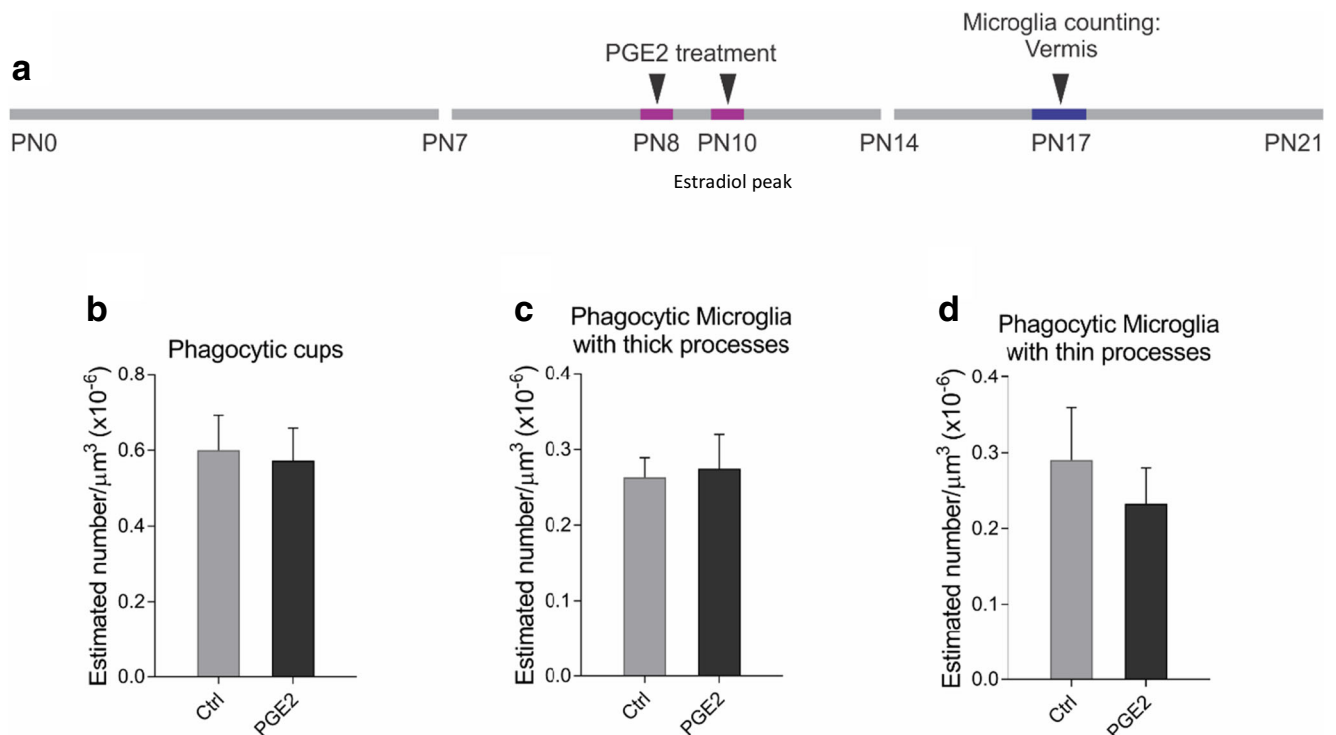


Fig. 6 Effect of PGE₂ infusion on microglial phagocytosis in the developing cerebellum. **a** Experimental design showing PGE₂ treatment interval (PN8 and PN10), and microglia counting at PN17 in the vermis. The number of phagocytic cups (**b**), phagocytic microglia with thick

processes (**c**), and phagocytic microglia with thin processes (**d**) counted in the vermis following treatment with PGE₂. Ctrl control, PGE₂ prostaglandin E₂, PN postnatal day

Experiment 7

qRT-PCR for Estrogen Receptors, Cyclooxygenases 1 and 2, and Microglial Phagocytosis Markers in the Developing Cerebellum

Using quantitative real-time PCR (qRT-PCR), we quantified *ERα* (*ESR1*) and *ERβ* (*ESR2*), *PTGS1* (*COX-1*), and *PTGS2* (*COX-2*) mRNA, as well as three phagocytic markers linked to microglia: *CD68* (cluster of differentiation 68), *LAMP1* (lysosomal-associated membrane protein 1), and *LAMP2*. Several time points before and after PN17 were examined to provide a better understanding of the expression of genes associated with prostaglandins, steroid hormones, and microglia phagocytosis. Frozen brain tissue was used to isolate RNA by disruption of tissue in Qiazol (Qiagen 79306) followed by binding to RNeasy columns (Qiagen 74104) with DNase digestion. cDNA was prepared from 1 μg of RNA using the Transcriptor First-Strand cDNA Synthesis Kit (Roche Applied Science 04897030001) using both anchored-dT and random primers. qRT-PCR was conducted on standards and samples run in triplicate using the SYBR green relative quantification method with a standard curve using an Applied Biosystems

ViiA7 with 384-well block. Specific primers for the genes *ERα*, *ERβ*, *COX-1*, *COX-2*, *CD68*, *LAMP1*, *LAMP2*, and *GAPDH* (control housekeeping gene) were designed using Primer Express v3.0 (Table 1).

Statistical Analysis

All data are expressed as mean ± SEM and effect size estimate calculations are also reported (η^2 and d). Data from experiment 1 was analyzed using a three-way ANOVA with region of the cerebellum, sex, and layer as fixed factors. Data from experiments 2 to 6 were analyzed using a two-way ANOVA with treatment and layer as fixed factors since no sex differences were found in experiment 1. Data from experiment 7 was analyzed using a one-way ANOVA with age as a fixed factor. Non-parametric tests Mann-Whitney *U* or Kruskal-Wallis were used when data did not comply with homogeneity of variance. All statistical analysis followed a post hoc pairwise comparison using the Holm's sequential Bonferroni correction to control for family-wise error. Significance was denoted when $p \leq 0.05$. All tests were computed in SPSS 24 and graphed in GraphPad Prism 7.

Table 1 Rat transcripts cDNA PCR primers

Gene	PubMed accession no.	Primer sequences	Amplicon length (bp)	Annealing temp (°C)
ESR1 (ER α)	NM_012689.1	F 5'—AAGGCTGCAAGGCTTCTTTAA R 5'—GGTTCTTATCGATGGTGCATTG	90	60
ESR2 (ER β)	NM_012754.1	F 5'—CCAACCTCCTGATGCTTCTTTCTC R 5'—GGACCACATTTTGCACCTTCATG	90	60
PTGS1 (COX-1)	NM_017043.4	F 5'—AAAGAACCCAATGTCCAGCAAG R 5'—GGCTCCCAACCAAAATCGTAG	152	60
PTGS2 (COX-2)	NM_017232.3	F 5'—TTCCAGTATCAGAACCGCATTG R 5'—GAGCAAGTCCGTGTTCAAGGA	151	60
CD68	NM_001031638.1	F 5'—ACACTTCGGGCCATGCTTCT R 5'—GATTGTCGTCTCCGGGTAACG	129	60
LAMP1	NM_012857.2	F 5'—AGACACACAATTCTTTCCCAATGC R 5'—CAGAGCACAATGGTCACATTCTTCA	144	60
LAMP2	NM_017068.2	F 5'—TTCTATCTGAAGGAAGTGAATGTCAACA R 5'—ACGGAAACCACCTGCTCTTTG	137	60
GAPDH	NM_017008.4	F 5'—TGGTGAAGGTCGGTGTGAACGG R 5'—TCACAAGAGAAGGCAGCCCTGGT	70	60

Results

Microglial Phagocytosis Is Higher in the Vermis Than in the Cerebellar Hemispheres

The statistical analysis detected a significant interaction between region and layer for phagocytic cups in the PN17 cerebellum [$F[2, 24] = 6.30, p = 0.006, \eta^2 = 0.344$]. The density of phagocytic cups was higher in the vermis than in the LH ($p = 0.002, d = 2.16$) and RH ($p = 0.006, d = 2.18$) (Fig. 2b). This difference was observed only in the GL. Likewise, a significant interaction between region and layer was detected for phagocytic microglia with thick processes [$F[2, 24] = 3.08, p = 0.06, \eta^2 = 0.20$]. The density of phagocytic microglia with thick processes was higher in the vermis than in the LH ($p = 0.036, d = 1.52$) and RH ($p = 0.009, d = 2.05$) in the GL, but not in the ML (Fig. 2c). Similar results were found for the density of phagocytic microglia with thin processes [$F[2, 24] = 4.76, p = 0.01, \eta^2 = 0.28$]. The vermis showed a higher density of phagocytic microglia with thin processes in the vermis compared to LH ($p = 0.02, d = 2.41$) and RH ($p = 0.04, d = 1.46$) (Fig. 2d). No significant effects were found for sex as a main factor or for the interaction between sex and region or sex and layer.

Treatment with Formestane Decreases the Number of Phagocytic Cups in the Vermis, but Not in the Cerebellar Hemisphere

We found a significant main effect of treatment in the vermis [$F[1, 48] = 13.735, p = 0.001, \eta^2 = 0.218$], where formestane decreased the number of phagocytic cups compared to control ($p = 0.044, d = 0.58$) (Fig. 3b). No effect of formestane on

phagocytic cups was seen in the cerebellar hemisphere [$F[1, 20] = 0.301, p = 0.590$] (Fig. 3c). We also found a significant interaction between treatment and region for phagocytic microglia with thin processes in the vermis [$F[1, 48] = 18.832, p = 0.000, \eta^2 = 0.282$] which were decreased by formestane treatment in the GL ($p = 0.01, d = 1.38$) and ML ($p = 0.015, d = 1.37$) (Fig. 3f). There was no effect of formestane on the density of phagocytic microglia with thin processes in the cerebellar hemisphere [$F[1, 20] = 0.000, p = 0.988$] (Fig. 3g). There was no effect of formestane treatment on phagocytic microglia with thick processes in the vermis (Fig. 3d) or the cerebellar hemisphere (Fig. 3e).

Treatment with Indomethacin or Nimesulide Also Decreases the Number of Phagocytic Cups in the Vermis, but Not in the Cerebellar Hemisphere

A significant interaction between treatment and layer was found for phagocytic cups in the vermis [$F[2, 30] = 3.65, p = 0.038, \eta^2 = 0.196$], where indomethacin and nimesulide treatment decreased the number compared to control ($p = 0.02, 1.74$). This effect was observed only in the ML (Fig. 4b). There was no effect of treatment in the hemispheres (Fig. 4c). Treatment with indomethacin and nimesulide impacted phagocytic microglia with thin processes in both the GL and ML of the vermis [$F[2, 30] = 4.11, p = 0.026, \eta^2 = 0.215$]. Treatment with Cox inhibitors decreased the density of phagocytic microglia with thin processes in the ML (indomethacin, $p = 0.007, d = 2.13$; nimesulide, $p = 0.037, d = 1.51$) compared to controls (Fig. 4f) and nimesulide concurrently increased the density of phagocytic microglia with thin processes in the GL ($p = 0.066, d = 1.30$; Fig. 4f), consistent with the anti-inflammatory effects of this Cox inhibitor. Once

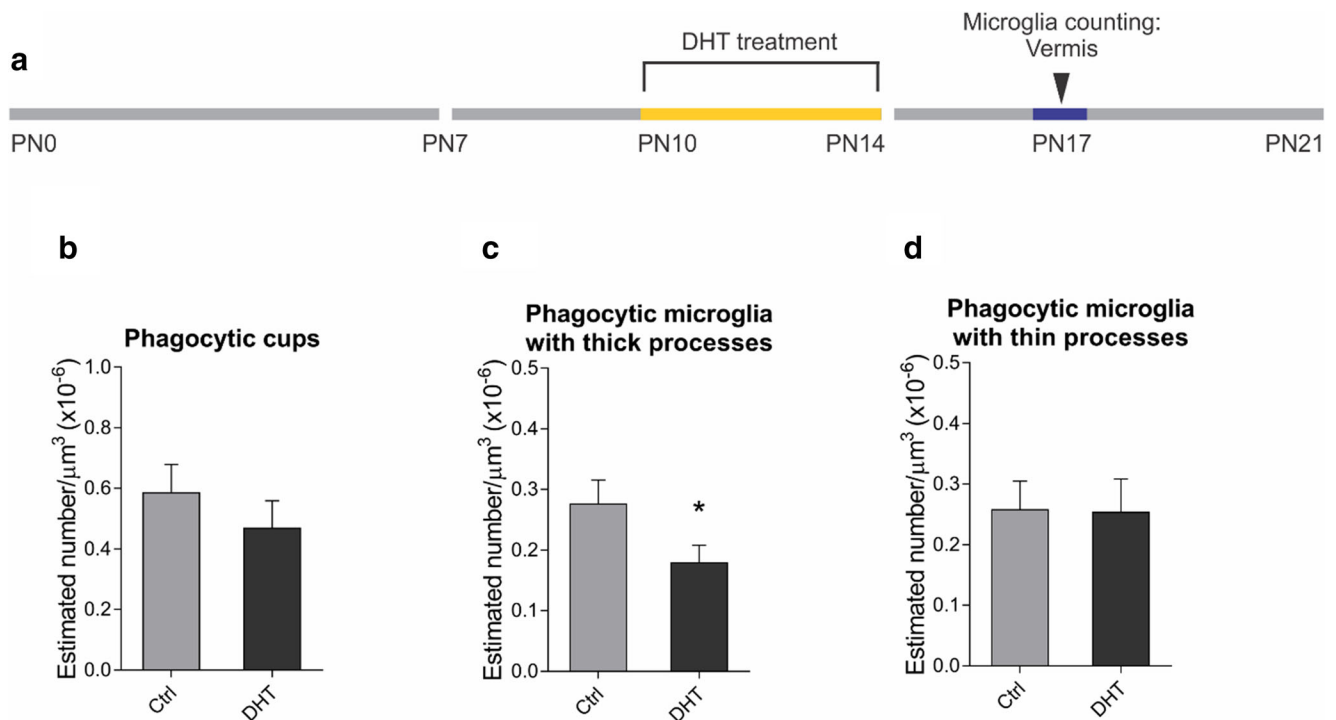


Fig. 7 Effect of DHT treatment on microglial phagocytosis in the developing cerebellum. **a** Experimental design showing DHT treatment interval (PN10–PN14), and microglia counting at PN17 in the vermis. Representation of the number of phagocytic cups (**b**), phagocytic

microglia with thick processes (**c**, $*p < 0.05$), and phagocytic microglia with thin processes (**d**) counted in the vermis following treatment with PGE₂. Ctrl control, PGE₂ prostaglandin E₂, PN postnatal day

again, there were no effects of treatment observed in the hemispheres (Fig. 4g) or on microglia with thick processes in either the vermis (Fig. 4d) or hemisphere (Fig. 4e).

Treatment with Exogenous Estradiol Has Only Modest Effects on Phagocytic Microglia

Treatment with estradiol from PN8 to PN10 did not significantly affect the number of phagocytic cups (Fig. 5b) or the density of phagocytic microglia with thick processes (Fig. 5c) in the vermis. Similarly, estradiol administration from PN10 to PN14 did not modify the number of phagocytic cups (Fig. 5f), the density of phagocytic microglia with thick (Fig. 5g), or phagocytic microglia with thin processes (Fig. 5h). However, estradiol treatment from PN8 to PN10 decreased the density of phagocytic microglia with thin processes ($U = 34.000$, $p = 0.028$; Fig. 5d).

Treatment with PGE₂ Had No Effect on Microglial Phagocytosis in the Developing Cerebellum

Treatment with PGE₂ had no effect on the number of phagocytic cups [$F[1, 20] = 0.091$, $p = 0.766$] (Fig. 6b) or the density of microglia with thick (Fig. 6c) or thin processes (Fig. 6d).

DHT Treatment Reduces Only Phagocytic Microglia with Thick Processes in the Developing Cerebellum

Treatment with DHT had no effect on the number of phagocytic cups ($U = 6.000$, $p = 0.126$; Fig. 7b). However, DHT treatment reduced the density of phagocytic microglia with thick processes in the vermis ($F[1, 18] = 5.363$, $p = 0.033$; Fig. 7c). No effects of DHT treatment were observed for phagocytic microglia with thin processes ($F[1, 18] = 0.006$, $p = 0.937$; Fig. 7d).

Patterns of mRNA Expression for Estrogen Receptors, Cyclooxygenases 1 and 2, and Phagocytic Markers

The statistical analysis detected a significant main effect of age for *ER α* mRNA [$F[4, 35] = 69.630$, $p = 0.000$] which significantly decreased on PN16 ($p = 0.001$, $d = 2.23$), PN17 ($p = 0.000$, $d = 4.61$), PN18 ($p = 0.000$, $d = 9.81$), and PN19 ($p = 0.000$, $d = 10.25$) compared to PN15 in the developing vermis (Fig. 8a). In contrast, *ER β* mRNA showed no significant change over time in the same region [$F[4, 35] = 2.260$, $p = 0.082$] (Fig. 8b). *COX-1* mRNA levels decreased during postnatal cerebellar development [$\chi^2 = 24.000$, $p = 0.000$], being lower on PN19 ($p = 0.021$) and PN21 ($p = 0.010$) compared to PN14, but not at PN17 (Fig. 8c). In contrast, *COX-2* mRNA levels increased as the cerebellum matured [$F[3, 28] = 20.131$, $p = 0.000$], being higher at PN17 ($p = 0.000$,

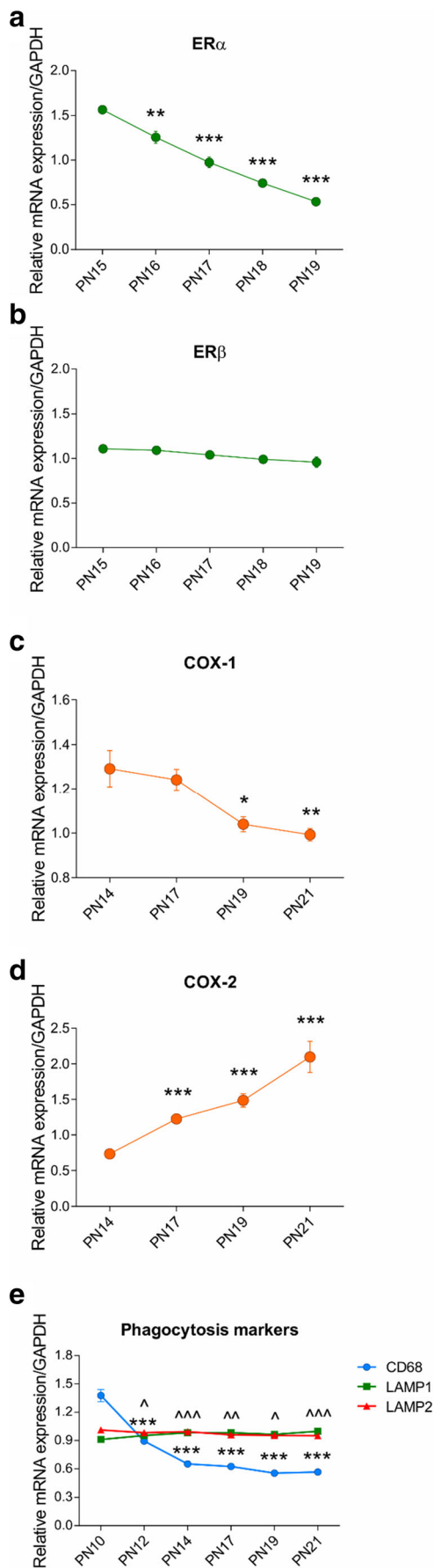


Fig. 8 Analysis of the mRNA expression for **a** *ER α* , **b** *ER β* , **c** *COX-1*, **d** *COX-2*, and **e** *CD68*, *LAMP1* and *LAMP2* in the rat cerebellum during the second and third postnatal weeks of development. Significant effects of ages were determined by comparing to the youngest age measured (* $p < 0.05$, ** $p < 0.01$, *** $p < 0.000$)

$d = 3.25$), PN19 ($p = 0.000$, $d = 3.70$), and PN21 ($p = 0.000$, $d = 3.20$) compared to PN14 (Fig. 8d). For *CD68*, its mRNA level changed as the cerebellum developed [$F[5, 39] = 87.465$, $p = 0.000$], with a significant decrease at PN12 ($p = 0.001$, $d = 3.83$), PN14 ($p = 0.000$, $d = 5.33$), PN17 ($p = 0.000$, $d = 5.77$), PN19 ($p = 0.000$, $d = 6.21$), and PN21 ($p = 0.000$, $d = 6.29$) when compared to PN10 (Fig. 8e). Likewise, the statistical analysis detected a significant effect for the lysosomal marker *LAMP1* [$F[5, 39] = 4.696$, $p = 0.002$] which decreased by PN12 ($p = 0.016$, $d = 1.46$), PN14 ($p = 0.000$, $d = 2.29$), PN17 ($p = 0.003$, $d = 1.89$), PN19 ($p = 0.062$, $d = 1.13$), and PN21 ($p = 0.000$, $d = 2.62$) compared to PN10 (Fig. 8e). There was no change with age in the levels of mRNA for lysosomal marker *LAMP2* (Fig. 8e).

Discussion

The human cerebellum matures postnatally and undergoes major growth and neuronal reorganization early in postnatal life [48, 51, 52]. In rats, the cerebellum matures during the first three postnatal weeks with important anatomical changes such as increased cell density and volume [49, 53]. Microglia phagocytosis during development is necessary to assemble and shape the brain. In the cerebellum, microglia promote the death of Purkinje cells [3] and are essential to the removal of apoptotic cells in a region- and age-dependent manner [5, 54]. We previously described the phagocytic profile of microglia in the developing rat cerebellar vermis in which we observed a peak in activity during the third postnatal week. Here we extend our study of microglial phagocytosis to the cerebellar hemispheres and find the vermis has higher microglial phagocytic activity than both cerebellar hemispheres. However, whether this developmental difference translates to a functional difference between the vermis and hemispheres still needs to be elucidated. We also extend our understanding of cerebellar development by exploring the role of prostaglandins and estrogen in microglia phagocytosis as these signaling molecules are essential to Purkinje cell maturation during the 2nd and 3rd postnatal weeks [20, 28, 29]. Treatment with inhibitors of the COX enzymes or aromatase significantly reduced phagocytic activity in the vermis but not in the hemispheres. Intriguingly, treatment with PGE₂ or estradiol itself had little or no effect, suggesting phagocytic activity in the developing cerebellum is intrinsically regulated and may be at an upper threshold. Treatment with the non-

aromatizable androgen, DHT, slightly reduced phagocytosis, consistent with the anti-inflammatory effects of androgens.

We previously reported that dysregulation of the PGE₂-estradiol pathway during the second postnatal week of development results in alterations of Purkinje dendritic trees and social play behavior in male rats [20, 28, 29]. Studies in vitro and under inflammatory conditions find that a reduction in PGE₂ levels, by COX-2 inhibitors, increases microglial phagocytosis [55]. Thus, PGE₂ plays a dual role as both a healthy developmental and inflammatory regulator in the brain. Our results may be relevant for neurodevelopmental disorders with an inflammatory component, microglia dysfunction, and cerebellar abnormalities such as autism spectrum disorders [56–61].

The phagocytic activity of microglia in the developing cerebellum peaks on PN17 [5], and mRNA levels for the aromatase gene, *Cyp19a*, peak in expression in the rat vermis around PN10 [28, 62]. Estrogen receptor alpha (ER α) is expressed by microglia in the adult mouse brain [63]. We found that blocking endogenous estradiol production reduced the overall number of phagocytic cups and phagocytic microglia with thin processes by ~50%. In contrast, treatment with estradiol only slightly impacted phagocytic microglia with thin processes with no effect on the number of phagocytic cups or phagocytic microglia with thick processes. We used a relatively low dose of estradiol in an attempt to remain in the physiological range but explored two different time points of exposure. Other studies have reported attenuated phagocytic activity of microglia after treatment with high doses of estradiol [64]. Steroids act through a variety of mechanisms which are often dose dependent. In other studies, estradiol's effects on microglial phagocytosis are independent of ER β activation under pathological conditions [65]. In this regard, we found the cerebellum expresses both *ER α* and *ER β* mRNA during the third postnatal week of development, with *ER α* more abundant than *ER β* , consistent with other studies [28, 66–69]. Whether the effects of estradiol on microglial phagocytosis in the developing cerebellum depend on its classical nuclear receptors remains to be determined. It is of interest that the gonadal hormones, estrogens and androgens, are modulators of cerebellar microglia phagocytic activity, yet we detected no effect of sex on any of the parameters measured. The developmental period for establishing sex differences in the rodent brain is earlier than that examined here, closer to the perinatal period [70], suggesting that sex hormones are potent regulators of brain development outside of and in addition to their role as drivers of brain sex differences.

Similar to the lack of effect of exogenous estradiol, we detected no effect of exogenous PGE₂ treatment during the second postnatal week of development. PGE₂ was delivered into the cisterna magna, at two time points before estradiol's peak at PN10 in a regime previously demonstrated by us to impact Purkinje cell dendritic maturation (Hoffman, Wright,

& McCarthy, 2016). This suggests both that the phagocytic profile is under tight and robust regulation and that it does not impact Purkinje cell maturation.

We also examined the mRNA of three phagocytosis markers associated with microglia: *LAMP1*, *LAMP2*, and *CD68* [71–73]. They were all expressed in the vermis during postnatal development. *LAMP1* and *LAMP2* showed a steady but overlapping expression pattern across the second and third postnatal week of development. *CD68*, however, gradually decreased from the second to the third postnatal week of life, consistent with an overall maturation of microglia.

Altogether, our study contributes to the understanding of the maturation of the cerebellum and implicates microglia as a participation in that process. We examined several aspects of the cerebellum's anatomy including the vermis and hemispheres, as well as its cortical layers and identified region specific developmental characteristics that should be considered in future studies of development of this key brain region. Future directions include determining how this microglial phagocytosis, in relation to sex hormones, regulates cerebellar development during the third postnatal week since cellular migration and dendritic growth are still happening at this time.

Conclusion

Microglia of the developing cerebellum exhibit a peak in phagocytic activity during the third postnatal week of development that is substantially higher in the vermis than the hemispheres and observed in both the GL and ML. Endogenous estrogens and prostaglandins upregulate this phagocytic activity in a region-dependent manner. The cellular and the molecular mechanisms by which estradiol or PGE₂ regulate microglial phagocytosis remain to be determined, but findings from this study highlight the critical role played by these endogenous signaling molecules which are readily modulated by common over-the-counter and prescriptions drugs.

Funding Information This work was supported by the NIH Grant R01-MH091424 to M.M.M.

Compliance with Ethical Standards

The Institutional Animal Care and Use Committee of the University of Maryland, Baltimore approved all animal procedures.

Conflict of Interest The authors declare that they have no competing interest.

References

1. Hong S, Stevens B. Microglia: phagocytosing to clear, sculpt, and eliminate. *Dev Cell*. 2016;38(2):126–8.

2. Schafer DP, Lehrman EK, Kautzman AG, Koyama R, Mardinly AR, Yamasaki R, et al. Microglia sculpt postnatal neural circuits in an activity and complement-dependent manner. *Neuron*. 2012;74(4):691–705.
3. Marin-Teva JL, Dusart I, Colin C, Gervais A, van Rooijen N, Mallat M. Microglia promote the death of developing Purkinje cells. *Neuron*. 2004;41(4):535–47.
4. Paolicelli RC, Bolasco G, Pagani F, Maggi L, Scianni M, Panzanelli P, et al. Synaptic pruning by microglia is necessary for normal brain development. *Science*. 2011;333(6048):1456–8.
5. Perez-Pouchoulen M, VanRyzin JW, McCarthy MM. Morphological and phagocytic profile of microglia in the developing rat cerebellum. *eNeuro*. 2015;2(4).
6. Kaur C, Sivakumar V, Zou Z, Ling EA. Microglia-derived proinflammatory cytokines tumor necrosis factor- α and interleukin-1 β induce Purkinje neuronal apoptosis via their receptors in hypoxic neonatal rat brain. *Brain Struct Funct*. 2014;219(1):151–70.
7. Lenz KM, Nugent BM, Haliyur R, McCarthy MM. Microglia are essential to masculinization of brain and behavior. *J Neurosci*. 2013;33(7):2761–72.
8. Weinhard L, di Bartolomei G, Bolasco G, Machado P, Schieber NL, Neniskyte U, et al. Microglia remodel synapses by presynaptic trogocytosis and spine head filopodia induction. *Nat Commun*. 2018;9(1):1228.
9. Swanson JA. Shaping cups into phagosomes and macropinosomes. *Nat Rev Mol Cell Biol*. 2008;9(8):639–49.
10. Schwarz JM, Sholar PW, Bilbo SD. Sex differences in microglial colonization of the developing rat brain. *J Neurochem*. 2012;120(6):948–63.
11. Wu CH, Wen CY, Shieh JY, Ling EA. A quantitative and morphometric study of the transformation of amoeboid microglia into ramified microglia in the developing corpus callosum in rats. *J Anat*. 1992;181(Pt 3):423–30.
12. Gomez-Gonzalez B, Escobar A. Prenatal stress alters microglial development and distribution in postnatal rat brain. *Acta Neuropathol*. 2010;119(3):303–15.
13. Sierra A, Encinas JM, Deudero JJ, Chancey JH, Enikolopov G, Overstreet-Wadiche LS, et al. Microglia shape adult hippocampal neurogenesis through apoptosis-coupled phagocytosis. *Cell Stem Cell*. 2010;7(4):483–95.
14. Ferrer-Martin RM, Martin-Oliva D, Sierra A, Carrasco MC, Martin-Estebane M, Calvente R, et al. Microglial cells in organotypic cultures of developing and adult mouse retina and their relationship with cell death. *Exp Eye Res*. 2014;121:42–57.
15. Abiega O, Beccari S, Diaz-Aparicio I, Nadjar A, Laye S, Leyrolle Q, et al. Neuronal hyperactivity disturbs ATP microgradients, impairs microglial motility, and reduces phagocytic receptor expression triggering apoptosis/microglial phagocytosis uncoupling. *PLoS Biol*. 2016;14(5):e1002466.
16. Nelson LH, Warden S, Lenz KM. Sex differences in microglial phagocytosis in the neonatal hippocampus. *Brain Behav Immun*. 2017;64:11–22.
17. Hong S, Dissing-Olesen L, Stevens B. New insights on the role of microglia in synaptic pruning in health and disease. *Curr Opin Neurobiol*. 2016;36:128–34.
18. Tremblay ME, Lowery RL, Majewska AK. Microglial interactions with synapses are modulated by visual experience. *PLoS Biol*. 2010;8(11):e1000527.
19. Grabert K, Michael T, Karavolos MH, Clohisey S, Baillie JK, Stevens MP, et al. Microglial brain region-dependent diversity and selective regional sensitivities to aging. *Nat Neurosci*. 2016;19(3):504–16.
20. Dean SL, Wright CL, Hoffman JF, Wang M, Alger BE, McCarthy MM. Prostaglandin E2 stimulates estradiol synthesis in the cerebellum postnatally with associated effects on Purkinje neuron dendritic arbor and electrophysiological properties. *Endocrinology*. 2012;153(11):5415–27.
21. Todd BJ, Schwarz JM, McCarthy MM. Prostaglandin-E2: a point of divergence in estradiol-mediated sexual differentiation. *Horm Behav*. 2005;48(5):512–21.
22. Amateau SK, McCarthy MM. A novel mechanism of dendritic spine plasticity involving estradiol induction of prostaglandin-E2. *J Neurosci*. 2002;22(19):8586–96.
23. McCarthy MM. Estradiol and the developing brain. *Physiol Rev*. 2008;88(1):91–124.
24. Sakamoto H, Mezaki Y, Shikimi H, Ukena K, Tsutsui K. Dendritic growth and spine formation in response to estrogen in the developing Purkinje cell. *Endocrinology*. 2003;144(10):4466–77.
25. Sasahara K, Shikimi H, Haraguchi S, Sakamoto H, Honda S, Harada N, et al. Mode of action and functional significance of estrogen-inducing dendritic growth, spinogenesis, and synaptogenesis in the developing Purkinje cell. *J Neurosci*. 2007;27(28):7408–17.
26. Bowers JM, Waddell J, McCarthy MM. A developmental sex difference in hippocampal neurogenesis is mediated by endogenous oestradiol. *Biol Sex Differ*. 2010;1(1):8.
27. Burks SR, Wright CL, McCarthy MM. Exploration of prostanoid receptor subtype regulating estradiol and prostaglandin E2 induction of spinophilin in developing preoptic area neurons. *Neuroscience*. 2007;146(3):1117–27.
28. Hoffman JF, Wright CL, McCarthy MM. A critical period in Purkinje cell development is mediated by local estradiol synthesis, disrupted by inflammation, and has enduring consequences only for males. *J Neurosci*. 2016;36(39):10039–49.
29. Dean SL, Knutson JF, Krebs-Kraft DL, McCarthy MM. Prostaglandin E2 is an endogenous modulator of cerebellar development and complex behavior during a sensitive postnatal period. *Eur J Neurosci*. 2012;35(8):1218–29.
30. Amateau SK, McCarthy MM. Induction of PGE2 by estradiol mediates developmental masculinization of sex behavior. *Nat Neurosci*. 2004;7(6):643–50.
31. Villa A, Vegeto E, Poletti A, Maggi A. Estrogens, neuroinflammation, and neurodegeneration. *Endocr Rev*. 2016;37(4):372–402.
32. Rivest S. Interactions between the immune and neuroendocrine systems. *Prog Brain Res*. 2010;181:43–53.
33. Woodling NS, Andreasson KI. Untangling the web: toxic and protective effects of neuroinflammation and PGE2 signaling in Alzheimer's disease. *ACS Chem Neurosci*. 2016;7(4):454–63.
34. Sarvari M, Kallo I, Hrabovszky E, Solymosi N, Liposits Z. Ovariectomy and subsequent treatment with estrogen receptor agonists tune the innate immune system of the hippocampus in middle-aged female rats. *PLoS One*. 2014;9(2):e88540.
35. Habib P, Beyer C. Regulation of brain microglia by female gonadal steroids. *J Steroid Biochem Mol Biol*. 2015;146:3–14.
36. Petrone AB, Simpkins JW, Barr TL. 17 β -estradiol and inflammation: implications for ischemic stroke. *Aging Dis*. 2014;5(5):340–5.
37. Chamniansawat S, Chongthammakun S. Inhibition of hippocampal estrogen synthesis by reactive microglia leads to down-regulation of synaptic protein expression. *Neurotoxicology*. 2015;46:25–34.
38. Siani F, Greco R, Levandis G, Ghezzi C, Daviddi F, Demartini C, et al. Influence of estrogen modulation on glia activation in a murine model of Parkinson's disease. *Front Neurosci*. 2017;11:306.
39. Minghetti L, Polazzi E, Nicolini A, Creminon C, Levi G. Up-regulation of cyclooxygenase-2 expression in cultured microglia by prostaglandin E2, cyclic AMP and non-steroidal anti-inflammatory drugs. *Eur J Neurosci*. 1997;9(5):934–40.
40. Minghetti L, Levi G. Microglia as effector cells in brain damage and repair: focus on prostanoids and nitric oxide. *Prog Neurobiol*. 1998;54(1):99–125.

41. Morale MC, Serra PA, L'Episcopo F, Tirolo C, Caniglia S, Testa N, et al. Estrogen, neuroinflammation and neuroprotection in Parkinson's disease: glia dictates resistance versus vulnerability to neurodegeneration. *Neuroscience*. 2006;138(3):869–78.
42. Hedges VL, Ebner TJ, Meisel RL, Mermelstein PG. The cerebellum as a target for estrogen action. *Front Neuroendocrinol*. 2012;33(4):403–11.
43. Tsutsui K. Neurosteroid synthesis and action in the cerebellum during development. *Cerebellum*. 2008;7(3):502–4.
44. Tai TC, Lye SJ, Adamson SL. Expression of prostaglandin E2 receptor subtypes in the developing sheep brainstem. *Brain Res Mol Brain Res*. 1998;57(1):161–6.
45. Kaufmann WE, Andreasson KI, Isakson PC, Worley PF. Cyclooxygenases and the central nervous system. *Prostaglandins*. 1997;54(3):601–24.
46. Paniagua-Herranz L, Gil-Redondo JC, Queipo MJ, Gonzalez-Ramos S, Bosca L, Perez-Sen R, et al. Prostaglandin E2 impairs P2Y2/P2Y4 receptor signaling in cerebellar astrocytes via EP3 receptors. *Front Pharmacol*. 2017;8:937.
47. Candelario-Jalil E, Slawik H, Ridelis I, Waschbisch A, Akundi RS, Hull M, et al. Regional distribution of the prostaglandin E2 receptor EP1 in the rat brain: accumulation in Purkinje cells of the cerebellum. *J Mol Neurosci*. 2005;27(3):303–10.
48. Butts T, Green MJ, Wingate RJ. Development of the cerebellum: simple steps to make a 'little brain'. *Development*. 2014;141(21):4031–41.
49. Goldowitz D, Hamre K. The cells and molecules that make a cerebellum. *Trends Neurosci*. 1998;21(9):375–82.
50. Bowers JM, Perez-Pouchoulen M, Roby CR, Ryan TE, McCarthy MM. Androgen modulation of Foxp1 and Foxp2 in the developing rat brain: impact on sex specific vocalization. *Endocrinology*. 2014;155(12):4881–94.
51. ten Donkelaar HJ, Lammens M, Wesseling P, Thijssen HO, Renier WO. Development and developmental disorders of the human cerebellum. *J Neurol*. 2003;250(9):1025–36.
52. Abraham H, Tomoczky T, Kosztolanyi G, Seress L. Cell formation in the cortical layers of the developing human cerebellum. *Int J Dev Neurosci*. 2001;19(1):53–62.
53. Heinsen H. Quantitative anatomical studies on the postnatal development of the cerebellum of the albino rat. *Anat Embryol*. 1977;151(2):201–18.
54. Ashwell K. Microglia and cell death in the developing mouse cerebellum. *Brain Res Dev Brain Res*. 1990;55(2):219–30.
55. He GL, Luo Z, Shen TT, Li P, Yang J, Luo X, et al. Inhibition of STAT3- and MAPK-dependent PGE2 synthesis ameliorates phagocytosis of fibrillar beta-amyloid peptide (1-42) via EP2 receptor in EMF-stimulated N9 microglial cells. *J Neuroinflammation*. 2016;13(1):296.
56. Theoharides TC, Asadi S, Patel AB. Focal brain inflammation and autism. *J Neuroinflammation*. 2013;10:46.
57. Vargas DL, Nascimbene C, Krishnan C, Zimmerman AW, Pardo CA. Neuroglial activation and neuroinflammation in the brain of patients with autism. *Ann Neurol*. 2005;57(1):67–81.
58. Pardo CA, Vargas DL, Zimmerman AW. Immunity, neuroglia and neuroinflammation in autism. *Int Rev Psychiatry*. 2005;17(6):485–95.
59. Rodriguez JI, Kern JK. Evidence of microglial activation in autism and its possible role in brain underconnectivity. *Neuron Glia Biol*. 2011;7(2–4):205–13.
60. Koyama R, Ikegaya Y. Microglia in the pathogenesis of autism spectrum disorders. *Neurosci Res*. 2015;100:1–5.
61. Takano T. Role of microglia in autism: recent advances. *Dev Neurosci*. 2015;37(3):195–202.
62. Lavaque E, Mayen A, Azcoitia I, Tena-Sempere M, Garcia-Segura LM. Sex differences, developmental changes, response to injury and cAMP regulation of the mRNA levels of steroidogenic acute regulatory protein, cytochrome p450scc, and aromatase in the olivocerebellar system. *J Neurobiol*. 2006;66(3):308–18.
63. Sierra A, Gottfried-Blackmore A, Milner TA, McEwen BS, Bulloch K. Steroid hormone receptor expression and function in microglia. *Glia*. 2008;56(6):659–74.
64. Bruce-Keller AJ, Keeling JL, Keller JN, Huang FF, Camondola S, Mattson MP. Antiinflammatory effects of estrogen on microglial activation. *Endocrinology*. 2000;141(10):3646–56.
65. Li R, Shen Y, Yang LB, Lue LF, Finch C, Rogers J. Estrogen enhances uptake of amyloid beta-protein by microglia derived from the human cortex. *J Neurochem*. 2000;75(4):1447–54.
66. Guo XZ, Su JD, Sun QW, Jiao BH. Expression of estrogen receptor (ER) -alpha and -beta transcripts in the neonatal and adult rat cerebral cortex, cerebellum, and olfactory bulb. *Cell Res*. 2001;11(4):321–4.
67. Price RH Jr, Handa RJ. Expression of estrogen receptor-beta protein and mRNA in the cerebellum of the rat. *Neurosci Lett*. 2000;288(2):115–8.
68. Shughrue PJ, Lane MV, Scrimo PJ, Merchenthaler I. Comparative distribution of estrogen receptor-alpha (ER-alpha) and beta (ER-beta) mRNA in the rat pituitary, gonad, and reproductive tract. *Steroids*. 1998;63(10):498–504.
69. Jakab RL, Wong JK, Belcher SM. Estrogen receptor beta immunoreactivity in differentiating cells of the developing rat cerebellum. *J Comp Neurol*. 2001;430(3):396–409.
70. McCarthy MM, Pickett LA, VanRyzin JW, Kight KE. Surprising origins of sex differences in the brain. *Horm Behav*. 2015;76:3–10.
71. Lynch MA. The multifaceted profile of activated microglia. *Mol Neurobiol*. 2009;40(2):139–56.
72. Pauwels AM, Trost M, Beyaert R, Hoffmann E. Patterns, receptors, and signals: regulation of phagosome maturation. *Trends Immunol*. 2017;38(6):407–22.
73. Fu R, Shen Q, Xu P, Luo JJ, Tang Y. Phagocytosis of microglia in the central nervous system diseases. *Mol Neurobiol*. 2014;49(3):1422–34.

Publisher's Note Springer Nature remains neutral with regard to jurisdictional claims in published maps and institutional affiliations.